JOURNAL OF MATERIALS SCIENCE 18 (1983) 3578–3590

Analytical technique for the determination of solidification rates during the inward freezing of cylinders

R. G. SANTOS, A. GARCIA
Faculty of Engineering, State University of Campinas (UNICAMP), Campinas, SP, Brazil

An analytical/experimental approach which permits the determination of solidification rates during the inward solidification of cylinders is proposed. The technique is based on a previous analytical solution that treats the generalized problem of solidification of slabs. This solution is modified by a geometric correlation to compensate for the cylindrical geometry. A number of experiments have been carried out with a special experimental set-up, designed to simulate the inward solidification of cylinders in a water-cooled mould. A series of comparisons of experimental results, numerical predictions and calculations furnished by the proposed technique were made, showing good agreement for any case examined.

Nomenclature

a_s Thermal diffusivity of solid metal $= k_s/c_s d_s$ ($m^2 sec^{-1}$).
A_i Internal surface area of the mould (m^2).
b_s Heat diffusivity of solid metal $= (k_s c_s d_s)^{1/2}$ ($J m^{-2} sec^{-1/2} K^{-1}$).
c_s Specific heat of solid metal ($J kg^{-1} K^{-1}$).
d_s Density of solid metal ($kg m^{-3}$).
h Newtonian heat transfer coefficient ($W m^{-2} K^{-1}$).
H Latent heat of fusion ($J kg^{-1}$).
k_s Thermal conductivity of solid metal ($W m^{-1} K^{-1}$).
q Heat flux ($W m^{-2}$).
r Radial position (m).
r_0 Radius of cylinder (m).
r_f Radius of solid/liquid interface (m).
S Thickness of solidified metal (m).
S_0 Thickness of metal side adjunct (m).
t Solidification time (sec).
T Temperature (K).
T_i Surface temperature (K).
T_f Freezing temperature of metal (K).
T_0 Temperature of the coolant (K).
T_s Temperature at any point in the solidified metal (K).
V_l Volume of remaining liquid metal during the solidification (m^3).
V_s Volume of solidified metal (m^3).
V_T Total volume of metal in the mould (m^3).
x Distance from metal/mould interface (m).
ϕ Dimensionless solidification constant.

1. Introduction

Transient heat-transfer problems involving solid/liquid phase change are important in many engineering applications such as the freezing of food [1], the formation of polar ice [2], the static and continuous casting of metals [3–5], welding [6], and many other operations [7]. The mathematical treatment of this problem is complicated by a non-linear boundary condition at the moving interface and by Newtonian heat transfer at the solid surface, and exact solutions are available for only a few special cases [8–17]. Techniques in which mathematical approximations are made, can be divided into analytical [2, 18–24] and numerical or graphical methods [25–32].

Under unidimensional heat flow conditions and in the case of a plane solid/liquid interface, the descriptions afforded by approximate models compare favourably with numerical predictions and experimental data [33]. However, for cylindrical

0022–2461/83 $03.00 + .12

or spherical geometries, the agreement observed between predictions furnished by the solutions proposed in the literature is not so good [21]. In such cases numerical solutions [25–32] have to be applied, although suffering from lack of generality and/or simplicity. Experimental data concerning these geometries are extremely rare in the literature. This is another point of difficulty when assessing the performance of different models.

The problem considered in this paper, is concerned with the inward solidification of a circular cylinder initially at the melting temperature with a coolant fluid outside the cylinder. The aim of the analysis is to present a new analytical approach to the problem that permits prediction of the position of the solid/liquid interface at any time as a function of the physical and geometric properties of the system. The evaluation of the proposed technique is made by comparing experimental results obtained in this work, with theoretical predictions furnished by the model and by other mathematical techniques representative of those existing in the literature.

2. Analysis

2.1. Theoretical considerations

The development of a mathematical model to describe solidification of cylinders is complicated by a number of factors. One of the most problematic of these is the difficulty of simultaneous treatment of heat flow through metal and mould by thermal conduction and across the metal/mould interface by Newtonian heat transfer. The solidification problem of a liquid metal at its freezing point inside a cylinder with coolant outside the cylinder can be adequately described by the following equation and boundary conditions:

$$\frac{\partial T}{\partial t} = \frac{k}{dc}\frac{1}{r}\frac{\partial}{\partial r}\left(r\frac{\partial T}{\partial r}\right), \quad r_f \leqslant r \leqslant r_0 \qquad (1a)$$

$$r_f = r_0, \text{ at } t = 0 \qquad (1b)$$

$$\frac{\partial r_f}{\partial t} = \frac{k}{dH}\frac{\partial T}{\partial r}, \text{ at } r = r_f \qquad (1c)$$

$$T = T_f, \text{ at } r = r_f \qquad (1d)$$

$$q = -k\frac{\partial T}{\partial r} = h(T_i - T_0), \quad r = r_0 \qquad (1e)$$

A physically realistic description of the problem involves the solution of Equation 1a using the boundary conditions given in Equations 1b to e. Mathematically exact solutions [8, 34] are limited to idealized situations mainly because they cannot incorporate the boundary condition in Equation 1e, which is a very strong restriction when considering a metal/mould system.

London and Seban [2] proposed an approximate solution with finite surface conductance (h), considering a linear temperature distribution over the solid thickness during solidification. This approximation gives good results for the analysis of rate of ice formation, but it is not appropriate for the solidification of metals. In the last case, the usual values of metal specific heats give rise to a curve temperature profile which makes the approximation inadequate. Analytical iteration methods can also be used to derive approximate solutions. Shih and Tsay [21] used the iteration method of Siegel and Savino [35, 36] to determine successive solutions for the instantaneous frozen layer thickness and temperature profile. These solutions take into account a constant heat transfer coefficient and neglect the heat capacity of the cylinder.

Tao [31] proposed a generalized numerical solution of the problem, where thermal conductivity, heat capacity of the solid phase and heat transfer coefficients are assumed to be constants. From this solution, the solid/liquid interface at any given time and the temperature profile at the instant of freezing at the centre, can be determined.

The above mentioned exact and approximate solution have hitherto been of very limited use due to their inability to take account respectively of imperfect thermal contact at the metal/mould interface, and solid heat capacity. Numerical techniques, on the other hand, can include both parameters and are versatile but have neither generality nor simplicity. A model that could provide a rapid and simple description of the inward solidification of a liquid inside a cylinder container would be of interest in industrial processes such as continuous casting of metals, freezing of food, production of ice, etc.

2.2. Model

The model to be discussed and evaluated here will be based on a previous analytical solution obtained by one of the present authors for slab-shaped bodies [16, 17]. In this model a virtual system is set up, in which the Newtonian resistance is represented by a pre-existing adjunct of material. The virtual coordinate system is displaced from the

real coordinate origin by the thickness of virtual adjunct introduced, as illustrated in Fig. 1.

The basic assumptions of the model are similar to those generally assumed when treating the solidification problem [9]. They are: (a) heat flow is geometrically unidimensional; (b) Newtonian interface resistance remains constant throughout the process; (c) thermal properties are independent of both position and time; (d) volume changes due to liquid and solid densities are neglected; (e) solidification occurs between the two constant temperatures of melt and coolant. In the virtual system the Fourier field equation is exactly applicable between the appropriate limits:

$$\frac{\partial T}{\partial t'} = \frac{k}{cd}\frac{\partial^2 T}{\partial x'^2},\ 0 \leqslant x' \leqslant S' \tag{2a}$$

The following boundary conditions are applicable to the virtual system:

$$T = T_f \text{ at } x' = S' \tag{2b}$$

$$T = T_0 \text{ at } x' = 0 \tag{2c}$$

$$\frac{dS'}{dt'} = \frac{k}{dH}\frac{\partial T}{\partial x'} \text{ at } x' = S' \tag{2d}$$

The Newtonian interfacial conductance (h) is taken into account by making an equivalence of heat flux between the real and virtual system at the beginning of solidification:

$$h(T_f - T_0) = k\left(\frac{\partial T}{\partial x'}\right)_{x' = S_0} \tag{3}$$

The solution is obtained in the virtual system and correlated to the real system by simple relationships, and is completely described by the following equations

$$t = \alpha S^2 + \beta S \tag{4}$$

$$T_s = T_0 + \frac{(T_f - T_0)}{\text{erf}(\phi)}\,\text{erf}\left(\phi\frac{\beta + 2\alpha x}{\beta + 2\alpha S}\right) \tag{5}$$

where

$$\alpha = \frac{1}{4a_s\phi^2} \tag{6a}$$

$$\beta = \frac{Hd_s}{h(T_f - T_0)}\,(= 2S_0\alpha) \tag{6b}$$

and ϕ may be obtained by iteration by:

$$\pi^{1/2}\phi\exp(\phi^2)\,\text{erf}(\phi) = \frac{c_s(T_f - T_0)}{H}\left(= \frac{1}{H^*}\right) \tag{7}$$

For slab-shaped and cylindrical geometries suitable non-dimensional variables are obtained by writing

$$t^* = \frac{h^2 t}{b_s^2},\ S^* = \frac{hS}{k_s} \tag{8}$$

Equation 4 can be modified to introduce these variables, assuming the following dimensionless form:

$$t^* = \frac{1}{4\phi^2}S^{*2} + H^*S^* \tag{9}$$

where

$$H^* = \frac{H}{c_s(T_f - T_0)} \tag{10}$$

In order to make possible comparison between the two geometries (see Fig. 2), it is convenient to define a correlation parameter which takes into account the volume of solidifying material and the

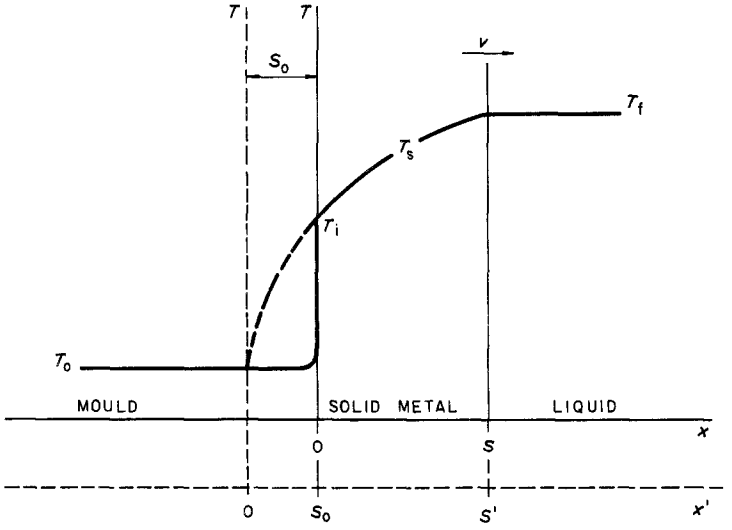

Figure 1 Real metal/mould system during the solidification in cooled moulds (full line) and correspondent virtual system (dashed line).

surface of heat exchange between material and coolant. That is

$$S^* = \left(\frac{V_s}{A_i}\right)^*_s \tag{11}$$

for slabs

and

$$\left(\frac{V_s}{A_i}\right)^*_c = \frac{(r_0^2 - r_f^2)h}{2r_0 k_s} \tag{12}$$

for cylinders.

Experimental evidence (see next section) has shown that the total solidification time of a cylinder is two times bigger than the corresponding time for the slab for the same value of V_s/A_i. By comparing a cylinder of radius r_0, with a slab of thickness $S = r_0$, and utilizing Equations 11 and 12, it follows that:

$$\frac{(V_s/A_i)^*_s}{(V_s/A_i)^*_c} = \frac{S}{(r_0^2 - r_f^2)/2r_0} \tag{13}$$

and at the end of solidification ($S = r_0, r_f = 0$), we have $(V_s/A_i)^*_s/(V_s/A_i)^*_c = 2$. This suggests that the above geometric correlation could be, in principle, a way to find a modifying factor to be applied in Equation 9 in order to enable this equation to cover the solidification of cylinders. On the other hand, it is known that differences in solidification times for the two geometries are small in the beginning of the process increasing up to the limiting value given by Equation 13 at the end of solidification. The variation from zero to this maximum value must be related to the volumes of solidified material and remaining liquid during the solidification process. For a slab of total thickness $S = r_0$, the ratio between volume of liquid and total volume of material in each time, is given by

$$\left(\frac{V_l}{V_T}\right)_s = \frac{(r_0 - S)}{r_0} \tag{14}$$

and for cylinders

$$\left(\frac{V_l}{V_T}\right)_c = \left(\frac{r_f}{r_0}\right)^2 \tag{15}$$

Equation 15 provides values ranging from one at the beginning of solidification ($r_f = r_0$) up to zero at the end of the process ($r_f = 0$), taking into account the decreasing volume to be solidified towards the centre of the cylinder. We can now define a test correction function based on a combination of Equation 13 evaluated at the end of solidification and Equation 15, given by:

$$\theta = \left[2 - \left(\frac{r_f}{r_0}\right)^2\right] \tag{16}$$

Fig. 3 shows the variation of the above function, for the slab-shaped and cylindrical geometries. Assuming that the function given by Equation 16 makes possible correction of solidification times of analogous slabs to cylinders, as it does at the beginning and end of solidification, we can write:

$$t^* = \left[2 - \left(\frac{r_f}{r_0}\right)^2\right]\left[\frac{1}{4\phi^2}\left(\frac{V_s}{A_i}\right)^{*2}_c + H^*\left(\frac{V_s}{A_i}\right)^*_c\right] \tag{17}$$

which gives the solidification time as a function of $(V_s/A_i)^*$ defined by Equation 12. The rate of solidification can be derived from Equation 17 and is given by:

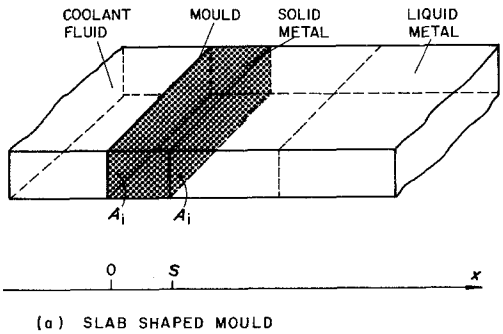

(a) SLAB SHAPED MOULD

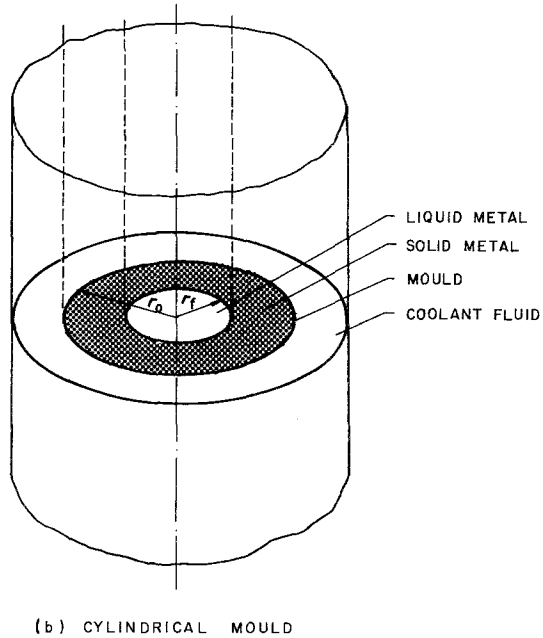

(b) CYLINDRICAL MOULD

Figure 2 Schematic illustration of the solidification in slab-shaped and cylindrical moulds.

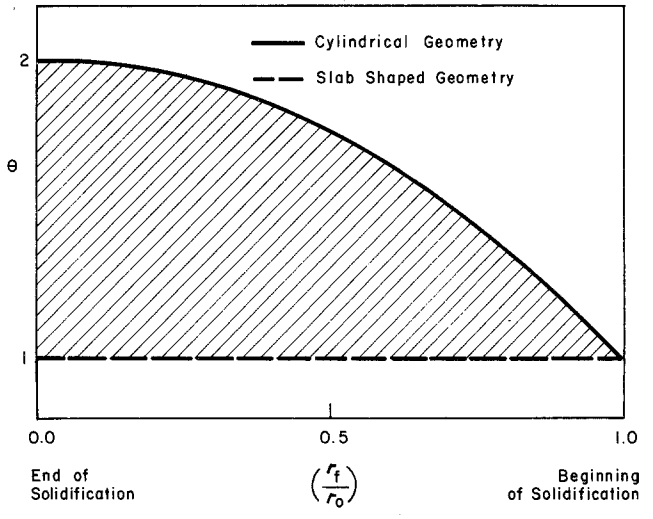

Figure 3 Variation of the function $\theta = [2-(r_f/r_0)^2]$ for slab-shaped and cylindrical moulds.

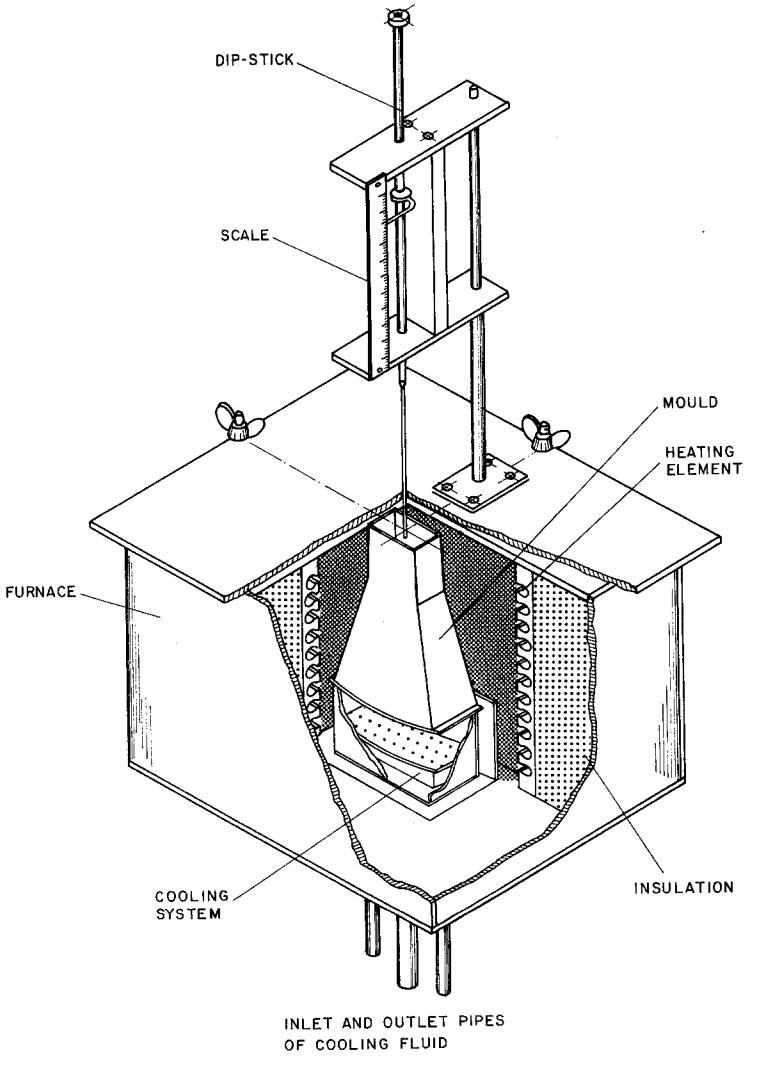

Figure 4 Experimental set-up used to simulate the inward solidification of a cylinder.

Figure 5 Macrostructure of a lead ingot showing the curvature of the solid/liquid interface due to a sudden change of solidification rate.

$$v = \left\{\frac{1}{C_2}\left(\frac{r_f}{r_0}\right)\left\{\left[\frac{C_1^2}{4\phi^2}\left(\frac{V_s}{A_i}\right)^2 + H^*C_1\left(\frac{V_s}{A_i}\right)\right]\frac{2}{r_0}\right.\right.$$
$$\left.\left. + \left[2 - \left(\frac{r_f}{r_0}\right)^2\right]\left[\frac{2C_1^2}{4\phi^2}\left(\frac{V_s}{A_i}\right) + H^*C_1\right]\right\}\right\}^{-1} \quad (18)$$

where

$$C_1 = \frac{h}{k_s} \text{ and } C_2 = \frac{h^2}{b_s^2} \quad (19)$$

3. Experimental details and discussion

The experimental examination of the inward solidification of cylinders was made by freezing aluminium, tin and lead against a water-cooled chill. The experimental set-up, shown in Fig. 4, was designed in order to simulate the inward solidification of a cylinder by detaching a volume element to represent the metal thermal behaviour. The curvature of the solid/liquid interface was checked by changing suddenly the cooling efficiency. Fig. 5 presents the macrostructure of a lead ingot showing the interface at the point where growth conditions were changed.

The position of the freezing front was monitored via the output of five fine thermocouples located respectively at 1, 5, 15, 30 and 40 mm from the metal/mould interface. A precision dipstick arrangement was also used to obtain information about the thickness. Repeated experiments showed that with thickness measurements accurate to ± 1.0 mm the measured times were reproducible to ± 2.0%. The dipstick measurements checked with temperature readings presented a maximum difference of 3.0%. Thermal measurements were also used to check difference of temperature along the melt. A maximum difference of about 1% of the melting point, was verified at 40 mm from the metal/mould interface for the case of aluminium solidified with a polished heat extracting surface.

The metal/mould conductance, characterized by the heat transfer coefficient, depends for a given metal/mould combination on the condition of mould surface. The heat flux between metal and mould is thus sensitive to mould surface microgeometry, the presence of mould coatings, etc. To investigate such influence, experiments were carried out under two sets of thermal contact conditions at the metal/mould interface: polished and coated with a thin layer of alumina ($\sim 100\,\mu m$). The values of heat transfer coefficients for each case were found by manipulation of growth data, as proposed in a previous article by one of the present authors [37]. The technique is based on the fact that at the beginning of solidification (in the limit $S \to 0$), heat flow and the kinetics of interface advance must in all cases be interface dominated. It is simply shown that in this regime the following equation must be applicable:

$$\frac{t}{S} = \frac{Hd}{h(T_f - T_0)} \quad (20)$$

The value of h obtained in this way will be that operative at the beginning of freezing. However for a vertical experimental configuration the interfacial heat transfer coefficient tends to remain unchanged during solidification, as the weight of the casting makes the contact pressure remain approximately constant. A best-fit iteration of growth data with numerical predictions was employed to evaluate heat transfer coefficients in order to compare them with measured values. Differences were never greater than ± 5% of the experimental value.

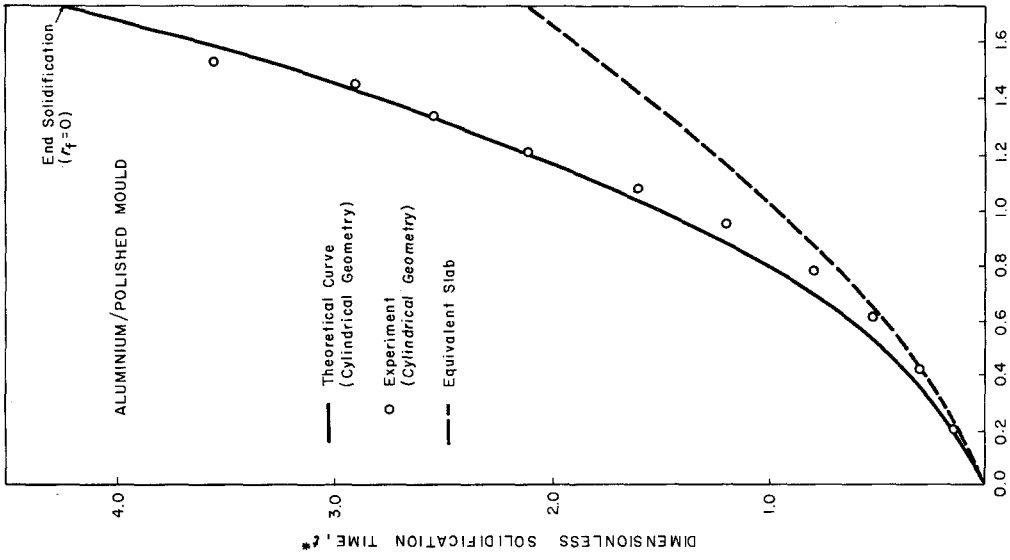

Figure 6 Comparison between experimental measurements and theoretical curves from the model (Equation 17).

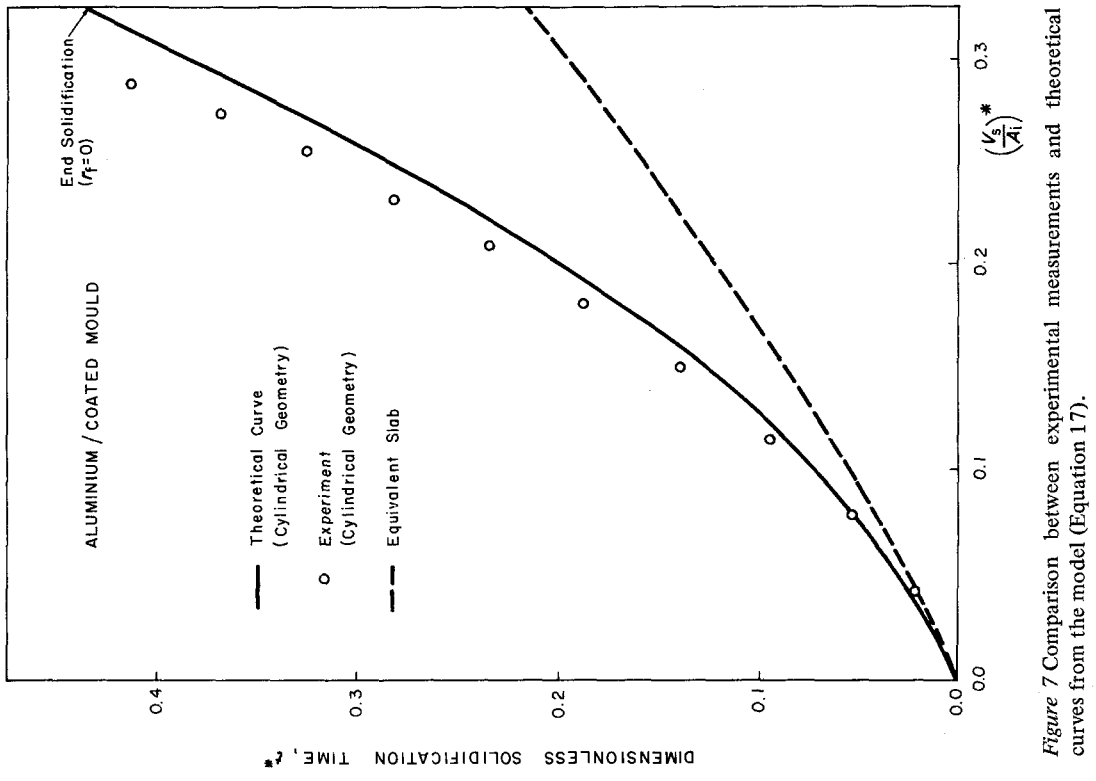

Figure 7 Comparison between experimental measurements and theoretical curves from the model (Equation 17).

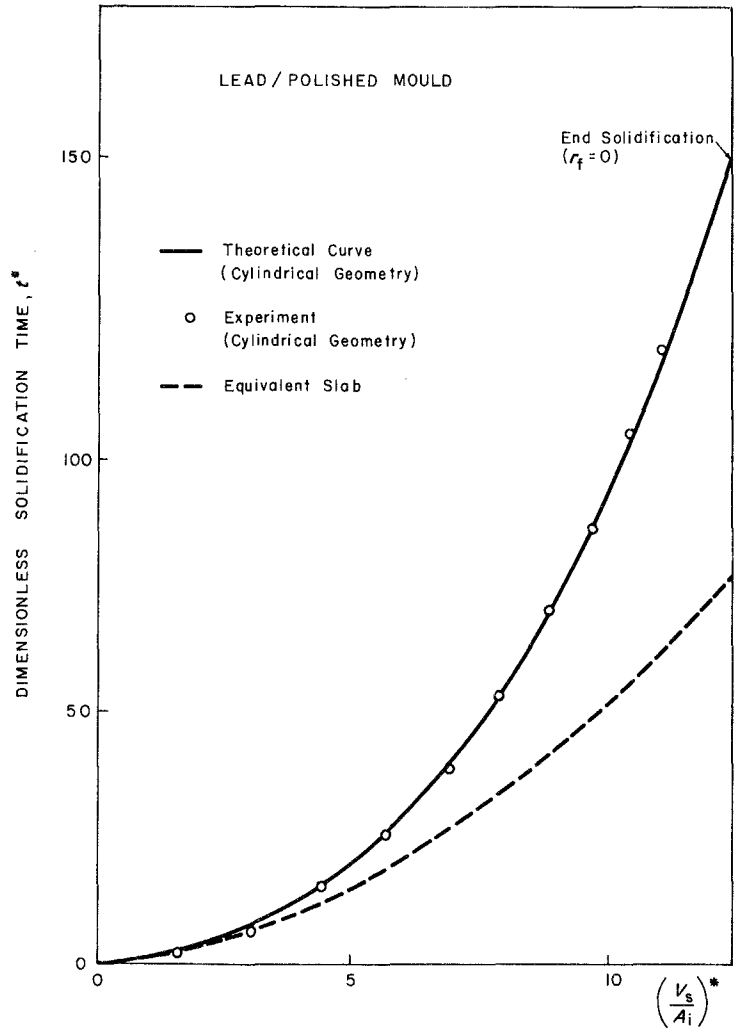

Figure 8 Comparison between experimental measurements and theoretical curves from the model (Equation 17).

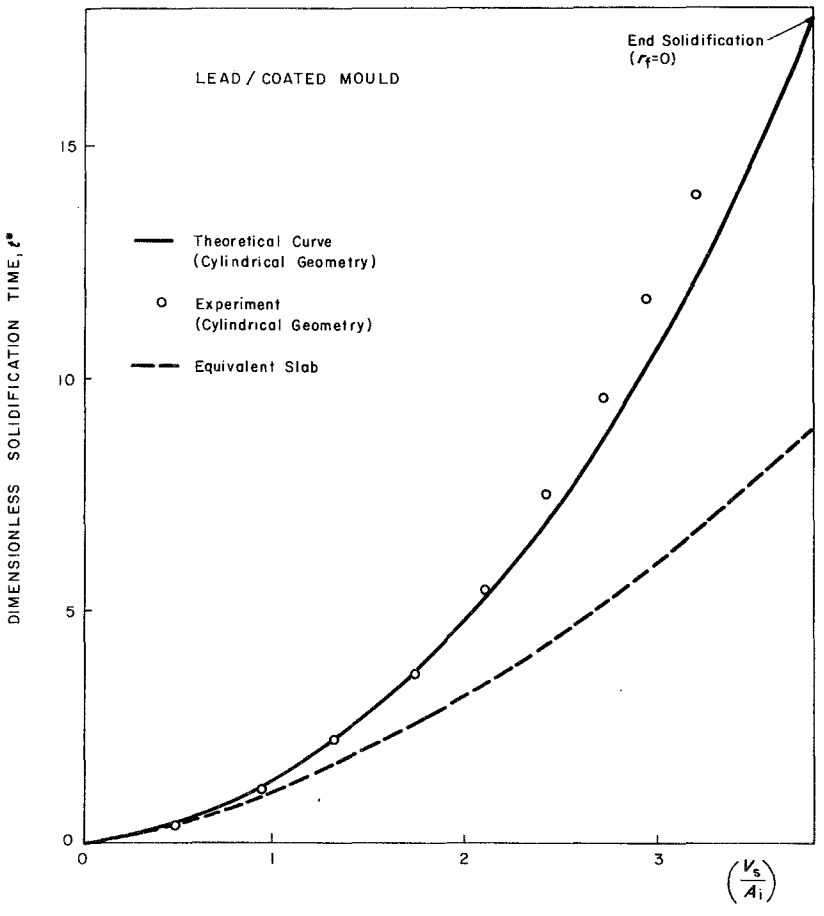

Figure 9 Comparison between experimental measurements and theoretical curves from the model (Equation 17).

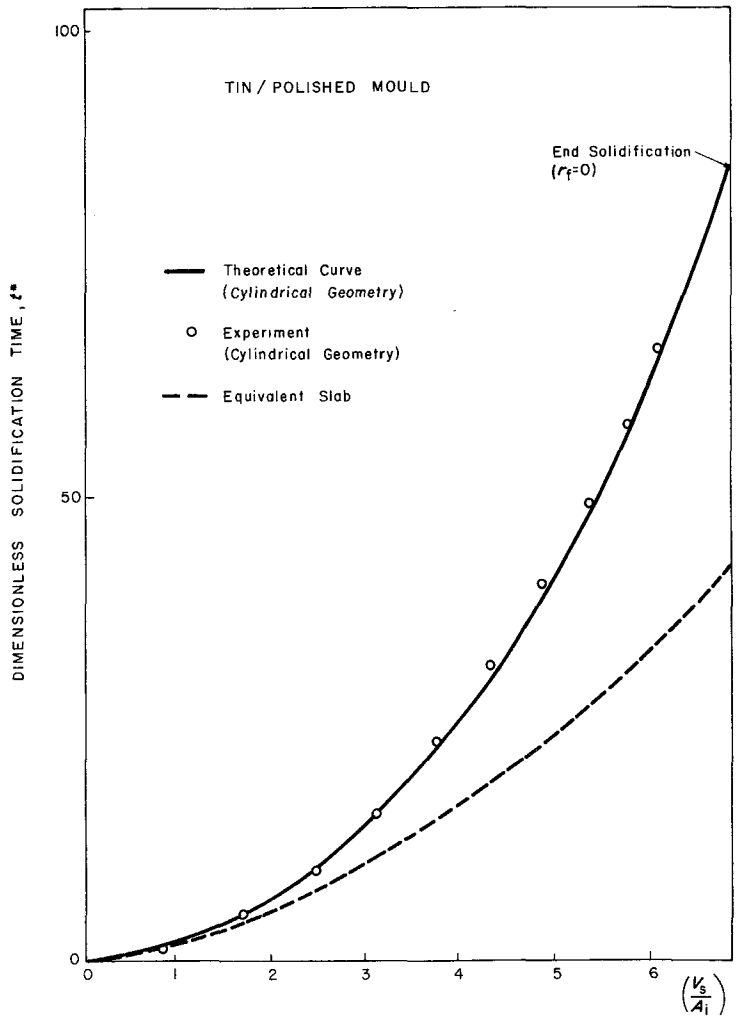

Figure 10 Comparison between experimental measurements and theoretical curves from the model (Equation 17).

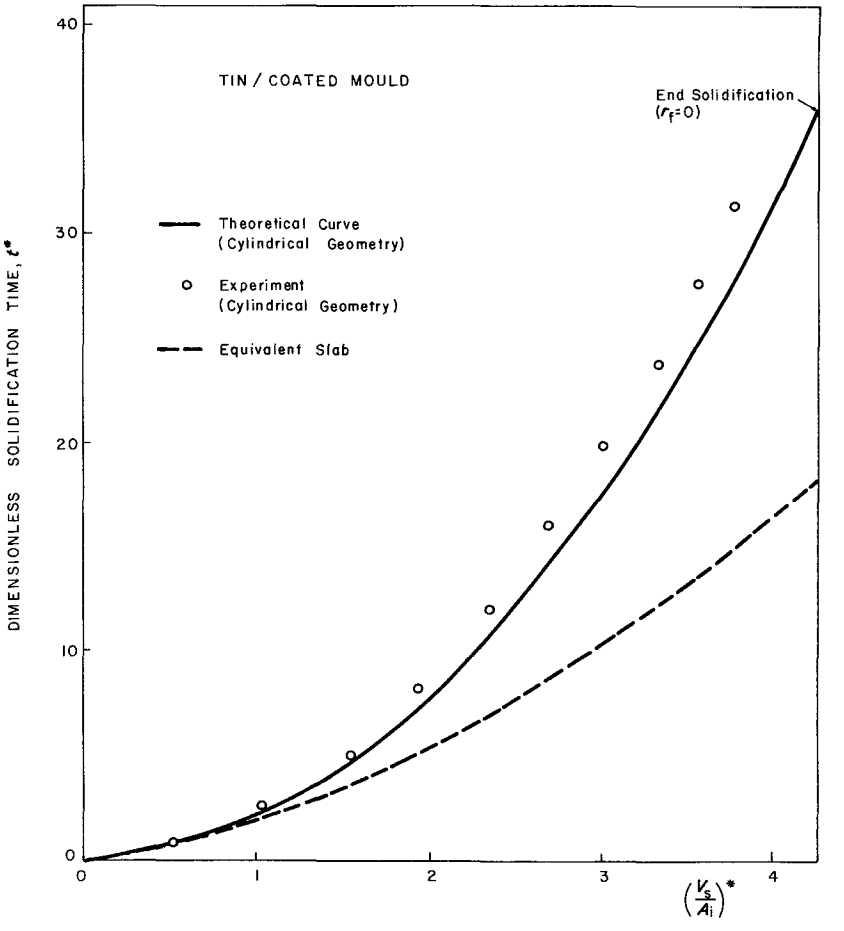

Figure 11 Comparison between experimental measurements and theoretical curves from the model (Equation 17).

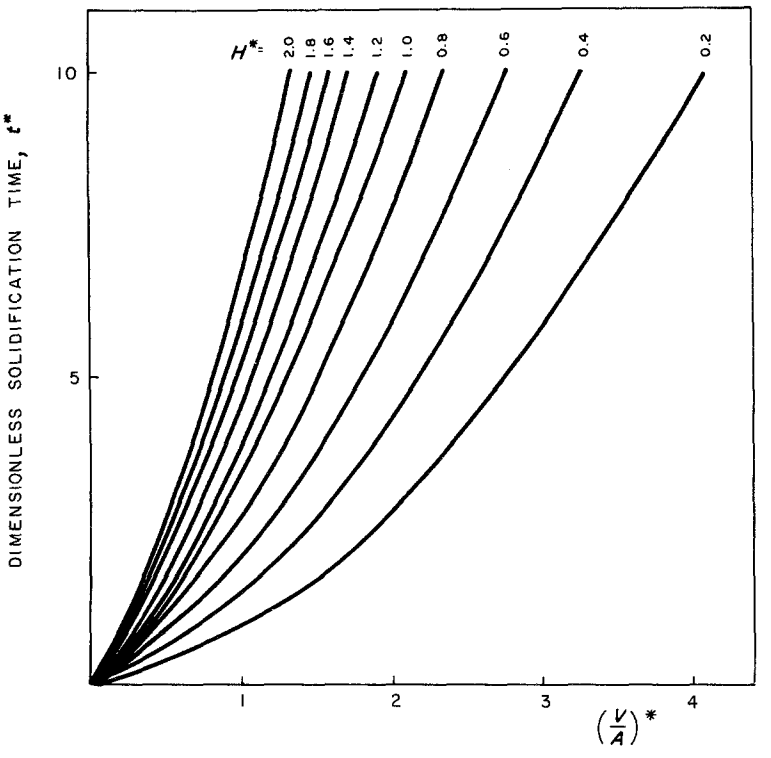

Figure 12 The dependence of thickness solidified on time given by Equation 17 for a range of dimensionless latent heat (H^*).

These differences introduce only minor errors when assessing the performance of different theoretical approaches.

Figs. from 6 to 11 show the experimental results obtained during the solidification of cylinders of aluminium, lead and tin (radius 0.15 m) respectively, converted to the dimensionless form by employing the appropriate value of the heat transfer coefficient. These are compared with the curves representing the predictions of the proposed technique. It can be seen that in any case examined predictions are close to the experimental curves. Fig. 12 shows a family of curves, given by Equation 17, where the dependence of thickness solidified on time is presented for a range of dimensionless latent heat values (H^*).

To assess the performance of the proposed model in comparison to the techniques existing in the literature, a comparison of predictions of different models is made in Figs. 13 and 14. This includes numerical and approximate treatments as well as the classical London and Seban analytical solution. It can be seen that the agreement observed between the numerical and proposed model is quite good over the range of conditions examined. The approximate solution by Shih and Tsay [21] presents only partial good agreement with experiment, and have a tendency to overestimate the time in the last third of the solidification process. The London and Seban [2] solution, as expected, does not furnish good predictions, because to neglect the heat capacity is a very strong restriction in the case of solidification of metals.

The proposed model can also be used to determine the rate of solidification. Fig. 15 presents predictions given by Equation 18, in comparison with experimental results for different metals, where good agreement is observed. A comparison can be made of the behaviour of different metals during solidification, by using Equation 18 on similar solidification conditions (Fig. 16).

4. Conclusions

A new technique describing the inward solidification of cylinders has been examined in particular and generalized cases. The generality of application of the model has been confirmed by comparison with the predictions of a finite difference numerical model. The proposed technique emerges as a useful tool in providing a rapid and simple description of the kinetics of freezing of cylinders for cases where thermal resistance of metal and metal/mould interface are of significance (mixed thermal control). The comparisons presented here have confirmed that a degree of confidence may

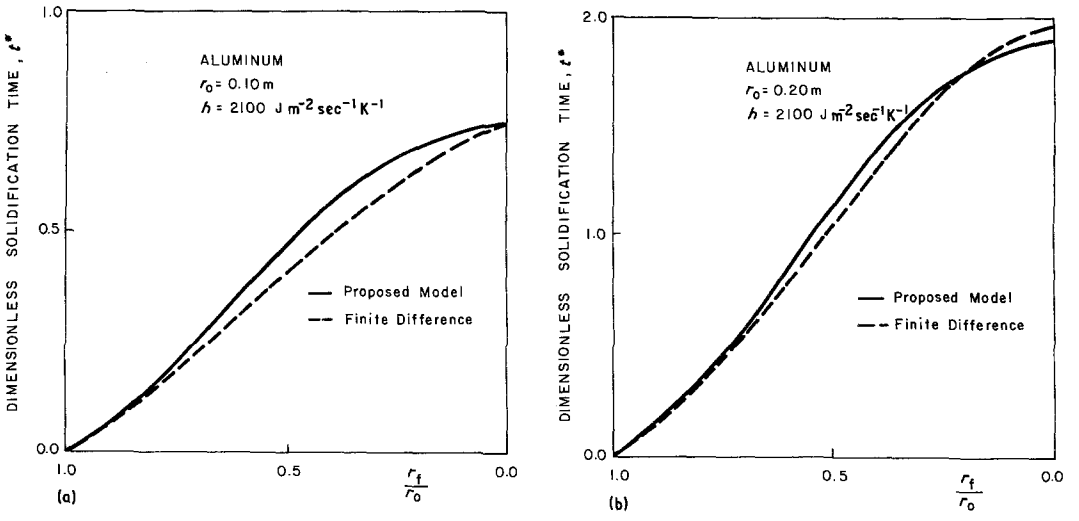

Figure 13 Comparison between proposed model (Equation 17) and a finite difference numerical model.

be placed in the predictions of the model under these circumstances. The technique has also proved to be useful in the determination of the rate of solidification of cylinders, with important consequences for the solidification structure and segregation aspects.

References

1. M. N. ÖZISIK, "Heat Conduction" (John Wiley and Sons, New York, 1980) pp. 397–438.
2. A. L. LONDON and R. A. SEBAN, *Trans. ASME* **65** (1943) 771.
3. T. W. CLYNE, A. GARCIA, P. ACKERMANN and W. KURZE, *J. Met.* **34** (1982) 34.

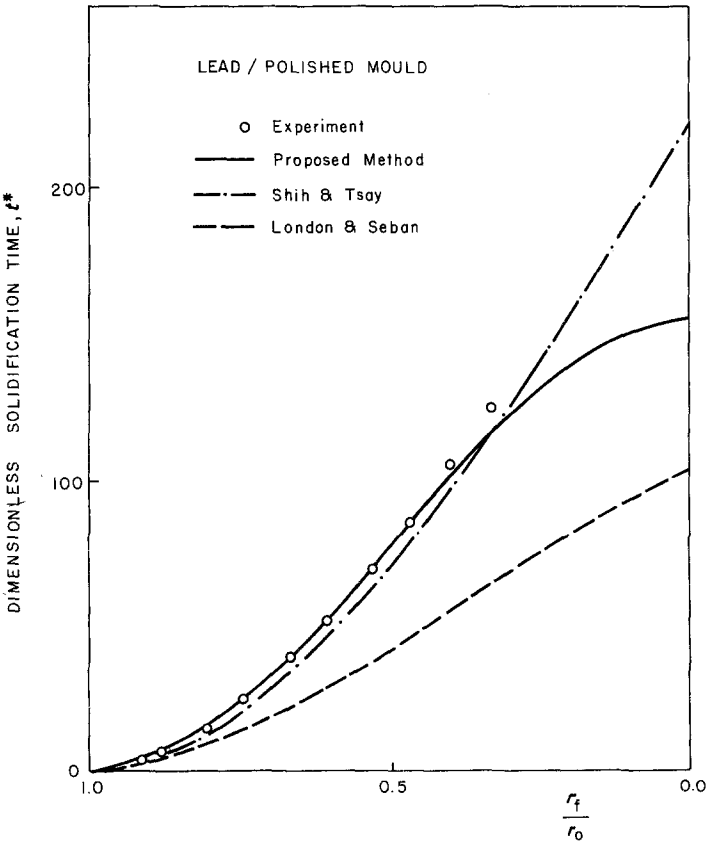

Figure 14 Comparison between the proposed method and other techniques existing in the literature.

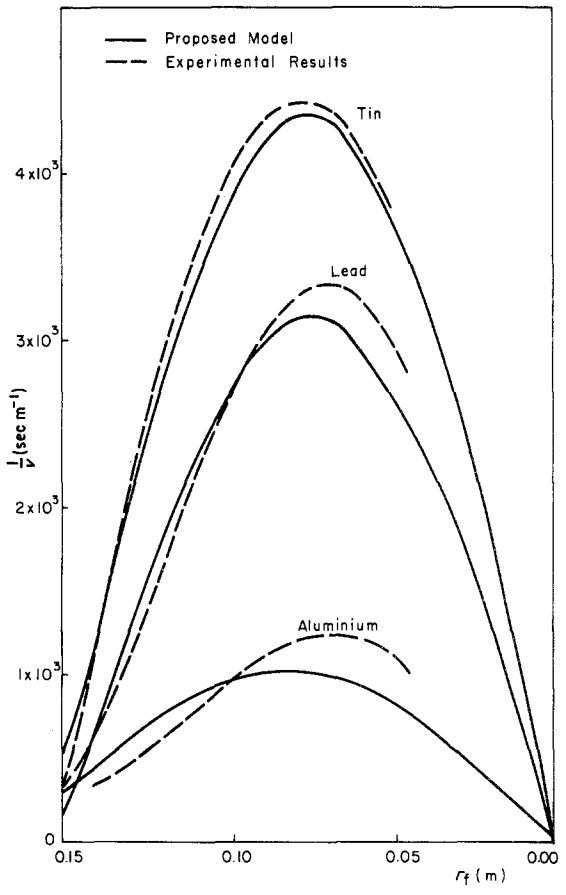

Figure 15 Comparison between the predictions given by Equation 18 and experimental results.

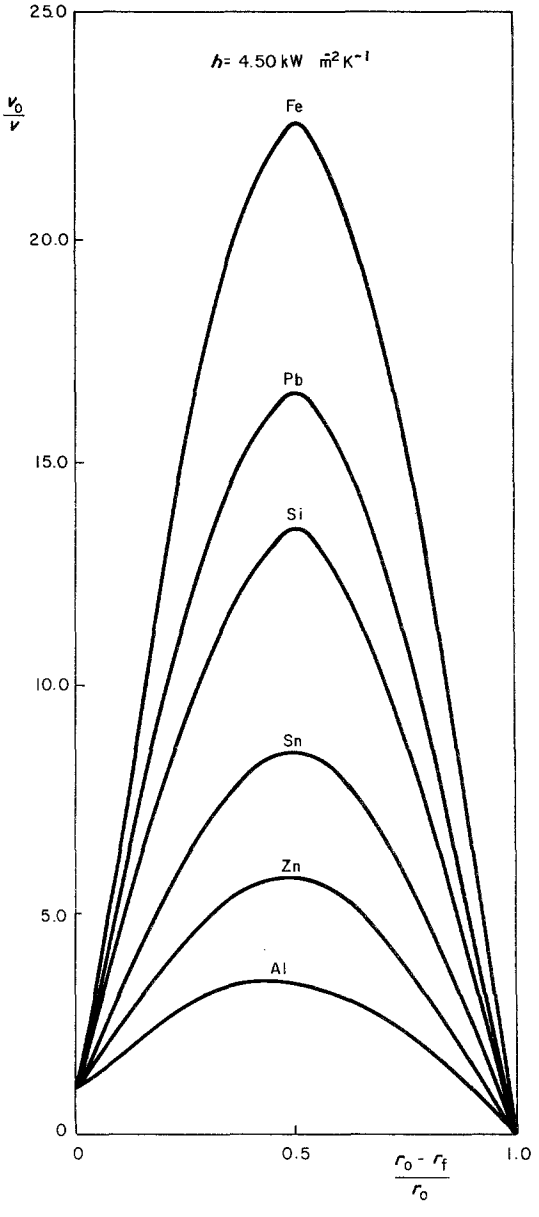

Figure 16 Comparison of solidification rates for different metals in cooled cylindrical moulds ($r_0 = 0.15$ m).

4. J. K. BRIMACOMBE, *Can. Met. Q.* **15** (1976) 1.
5. J. K. BRIMACOMBE, J. E. LAIT and F. WEINBERG, "Mathematical Process Models" (The Metals Society, London, 1974).
6. W. F. SAVAGE, C. D. LUNDIN and A. H. ARONSON, *Welding J. (Research Suppl.)* **44** (1965) 175-s.
7. T. W. CLYNE and A. GARCIA, *J. Mater. Sci.* **16** (1981) 1643.
8. H. S. CARSLAW and J. C. JAEGER, "Conduction of Heat in Solids" (Oxford University Press, London, 1959) pp. 282–296.
9. R. W. RUDDLE, "The Solidification of Castings" (The Institute of Metals, London, 1957) pp. 72–120.
10. G. H. GEIGER and D. R. POIRIER, "Transport Phenomena in Metallurgy" (Addison Wesley, Massachussetts, 1973) pp. 329–360.
11. N. M. H. LIGHTFOOT, *Proc. London Math. Soc.* **31** (1930) 97.
12. C. SCHWARTZ, *Zeitschrift für Angereandt Mathematik und Mechanik* **13** (1933) 202.
13. Y. LYUBOV, *Doklay Akad. Nauk SSSR* **68** (1949) 847.
14. J. STEFAN, *Ann. Phys. u Chem.* **42** (1891) 139.
15. N. CHVORINOV, *Die Giesserei* **27** (1940) 177.
16. A. GARCIA and M. PRATES, *Met. Trans. B* **9** (1978) 449.
17. A. GARCIA, T. W. CLYNE and M. PRATES, *ibid.* **10** (1979) 85.
18. C. M. ADAMS Jr, "Liquid Metals and Solidification" (American Society for Metals, Cleveland, 1958) pp. 187–217.
19. A. W. D. HILLS, *Trans. TMS-AIME* **245** (1969) 1471.
20. P. HRYCAK, *A.I.Ch.E.J.* 9 (1963) 585.
21. Y. P. SHIH and S. Y. TSAY, *Chem. Eng. Sci.* **26** (1971) 809.
22. Y. P. SHIH and T. C. SHOU, *ibid.* **26** (1971) 1787.
23. D. S. RILEY, F. T. SMITH and G. POOTS, *Int. J. Heat Mass Transfer* **17** (1974) 1507.

24. J. KERN and G. L. WELLS, *Met. Trans. B* 8 (1977) 99.
25. P. A. LONGWELL, *A.I.Ch.E.J.* 4 (1958) 53.
26. G. M. DUSIMBERRE and V. A. BLACKSBURG, *Trans. ASME* 67 (1945) 703.
27. R. J. SARJANT and M. R. SLACK, *J. Iron Steel Inst.* 177 (1954) 428.
28. D. C. BAXTER, *J. Heat Transfer* 84 (1962) 317.
29. J. SCHNIEWIND, *J. Iron Steel Inst.* **201** (1963) 594.
30. J. G. HENZEL Jr and J. KEVERIAN, *Trans. AFS* 74 (1965) 661.
31. L. C. TAO, *A.I.Ch.E.J.* **13** (1967) 165.
32. *Idem, ibid.* **14** (1968) 720.
33. T. W. CLYNE and A. GARCIA, *Int. J. Heat Mass Transfer* **23** (1980) 773.
34. M. N. ÖZISIK and J. C. UZZELL Jr, *J. Heat Transfer* **101** (1979) 331.
35. R. SIEGEL and J. M. SAVINO, *Proc. 3rd Heat Transfer Conf., Amer. Soc. Mech. Eng.* 4 (1966) 141.
36. *Idem, Int. J. Heat Mass Transfer* **12** (1969) 803.
37. A. GARCIA and T. W. CLYNE, "Solidification Technology in the Foundry and Casthouse" (Metals Society, London, 1983) p. 33.

Received 1 December 1982
and accepted 23 March 1983